# Polymer Films Removed from Solid Surfaces by Nanostructured Fluids: Microscopic Mechanism and Implications for the Conservation of Cultural Heritage

Martina Raudino, Giulia Selvolini, Costanza Montis, Michele Baglioni,[†] Massimo Bonini, Debora Berti,* and Piero Baglioni*[,†]

Department of Chemistry and CSGI, University of Florence, Via della Lastruccia 3, 50019 Sesto Fiorentino, Florence Italy

ABSTRACT: Complex fluids based on amphiphilic formulations are emerging, particularly in the field of conservation of works of art, as effective and safe liquid media for the removal of hydrophobic polymeric coatings. The comprehension of the cleaning mechanism is key to designing tailored fluids for this purpose. However, the interaction between nanostructured fluids and hydrophobic polymer films is still poorly understood. In this study, we show how the combination of confocal laser scanning microscopy (CLSM) and atomic force microscopy (AFM) provides interesting and complementary insight into this process. We focused on the interaction between an ethyl methacrylate/methyl acrylate 70:30 copolymer film deposited onto a glass surface and a water/nonionic surfactant/2-butanone (MEK) ternary system, with MEK being a good solvent and water being a nonsolvent for the polymer. Our results indicate a synergy between the organic solvent and the surfactant assemblies: MEK rapidly swells the outer layers of the polymer film allowing for the subsequent diffusion of solvent molecules, while the amphiphile decreases the interfacial energy between the polymeric coating and the liquid phase, favoring dewetting and dispersion of swollen polymer droplets in the aqueous phase. The chemical nature of the surfactant and the microstructure of the assemblies determine both the kinetics and the overall efficiency of polymer removal, as assessed by comparing the behavior of similar formulations containing an anionic surfactant (sodium dodecyl sulfate, SDS).

KEYWORDS: nanostructured fluids, polymer film, detergency, dewetting, conservation cultural heritage, confocal microscopy, atomic force microscopy, small angle X-ray scattering
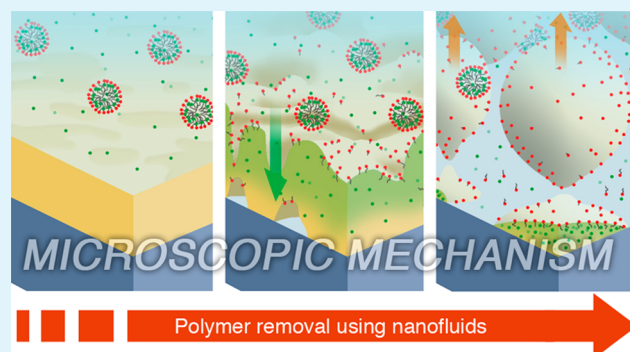
1. INTRODUCTION

The interaction of complex fluids with polymeric films is of central interest for all the processes where wetting and adhesion phenomena are involved. A prominent field of application is represented by conservation science. Until recently, synthetic polymers have been widely used as fixatives, protective agents, and adhesives in the conservation of works of art and, in particular, of wall paintings.[1] However, these polymeric coatings decrease the permeability of the substrate to liquid and gaseous water. Soluble salts, that are ubiquitous in walls, are therefore forced to crystallize inside the wall porous matrix below the pictorial layer, rather than on its surface, causing strong mechanical stresses and eventually leading to the loss of the works of art.[2] In addition, the photo-oxidative degradation of the polymer can lead to the yellowing of the coating and/or to the formation of insoluble fractions of polymer, which makes the treatment irreversible.[3]

The selective removal of polymeric coatings is therefore one of the main challenges in conservation science. Neat organic solvents have been traditionally used for this purpose. However, besides the not negligible toxicity of several organic solvents,

their action is scarcely controllable: in particular, when working on porous matrixes, the dissolved polymer spreads and redeposits deep into the pores.

Nanostructured cleaning media, such as micellar solutions and oil-in-water (o/w) microemulsions, have gained growing attention in recent years as a safe alternative to overcome these issues.[4,5] These formulations are composed of water (75−95%), oil (2−20%), and surfactants (3−5%). By "oil", we define one or more organic solvents, sometimes partially miscible with water, chosen among the good solvents for the polymer that has to be removed. The aqueous bulk phase ensures controlled penetration and environmental safety; the relatively small percentages of oil allow the removal of the polymer, which is swollen and detached from the surface. Even in the presence of good solvents miscible with water, the presence of surfactant assemblies greatly enhances the cleaning effectiveness and is necessary for polymer detachment.[6,7]

This recent scientific field is strongly oriented toward practical applications, and a fairly high number of novel formulations are nowadays tested on fresco paintings treated with different polymers.[8−10] As a consequence, a formulation palette is already available, but the knowledge on the fundamental aspects of this phenomenon is still limited. The simultaneous presence of surfactant assemblies and of a good solvent is necessary in all the case studies, but much less is known about the exact mechanism that endows a particular formulation with superior performances with respect to apparently similar fluids. Until present, the role of each component and the key steps occurring during the interaction between the fluid and the polymeric film are far from being clarified, mostly due to the numbers of variables, i.e., chemical nature of the components, microstructure, substrate nature, polymer nature, aging of the coating, environmental conditions, etc.

For a better comprehension of this mechanistic aspect, we report here on a model system where a polymer film of controlled and homogeneous thickness is applied onto a glass surface and challenged with complex fluids of known composition and microstructure. The use of glass substrates provides a simple model surface coated with films with very reproducible thickness and structure, where roughness and surface morphology before exposure to the nanofluid can be neglected. Moreover, despite its simplicity, this model substrate is representative of wall paintings produced in the laboratory and "real" frescoes treated with acrylic copolymers.[8] In particular, a coating of ethyl methacrylate/methyl acrylate 70:30 copolymer (marketed as Paraloid B72 and one of the most used synthetic polymers in conservation of cultural heritage) was put in contact with an amphiphilic formulation containing water, 2-butanone (MEK, i.e., a good solvent for acrylic polymers), and a nonionic surfactant ($C_{9−11}E_6$, an ethoxylated alcohol with a broad homologue distribution, hereafter referred to as BR[8], for "broad range"). This formulation efficiently removes Paraloid B72 coatings from laboratory models and on real frescoes.[11]

The molecular mechanism of the removal process is investigated by combining confocal laser scanning microscopy and atomic force microscopy. In order to stress the synergistic role of the amphiphilic assemblies and of the organic solvent, we compare this ternary system to water/MEK mixtures and aqueous solutions of the nonionic surfactant. The comparison with similar formulations, containing the anionic surfactant sodium dodecyl sulfate (SDS), addresses the effect of the chemical nature of the surfactant and of the structure of the fluid at the nanoscale. Water/SDS/MEK systems were included as reference, because SDS-based formulations have been commonly used in the past for conservative purposes and have been among the best performing system so far developed.[6,12] These formulations are particularly interesting thanks to the good emulsifying power and the excellent detergency properties of SDS, which also forms stable o/w microemulsions in the presence of small amounts of a cosurfactant.

2. EXPERIMENTAL SECTION

2.1. Chemicals. BR ethoxylated alcohol (AkzoNobel, purity 98%), sodium dodecyl sulfate (SDS, Sigma-Aldrich, purity 99%), 2-butanone (MEK, Sigma-Aldrich, purity 99%), ethyl acetate (Sigma-Aldrich, ACS reagents, purity ≥99.5%), and fluorescent probes used for confocal laser scanning microscopy (CLSM) experiments (Rhodamine 110

chloride and Rhodamine B isothiocyanate, Sigma-Aldrich, purity >99%) were used without further purification (see Figure 1 for
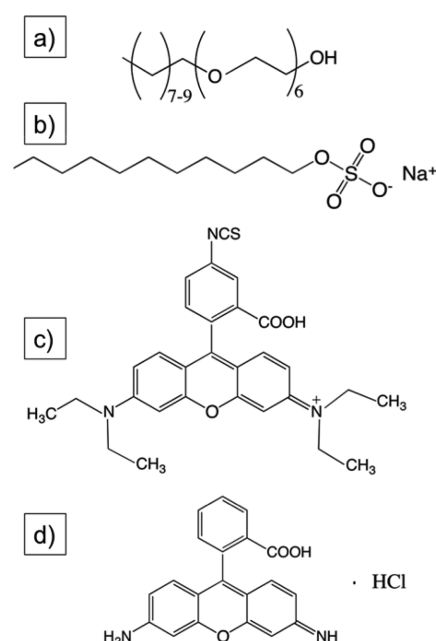

Figure 1. Structure of the used chemicals: (a) BR surfactant, (b) sodium dodecyl sulfate, (c) Rhodamine B isothiocyanate, and (d) Rhodamine 110 chloride.

chemical structures). Water was purified with a Millipore Milli-Q gradient system (resistivity >18 MΩ cm). Paraloid B72 pellets were purchased from Zecchi, Florence, and dissolved in ethyl acetate to obtain a solution 10% w/w.

2.2. Samples Preparation. Water/MEK and water/surfactants micellar solutions were prepared mixing the components under stirring. For the ternary samples, MEK was added to the micellar solutions of BR or SDS surfactant under constant stirring. Table 1 reports the chemical composition of all the investigated samples.

Table 1. Chemical Composition of the Cleaning Fluids

	composition (% w/w)		
sample	water	surfactant	MEK
H_2O/MEK	80		20
BR/MEK 0%	95	5	
SDS/MEK 0%	95	5	
BR/MEK 20%	76	4	20
SDS/MEK 20%	76	4	20

For CLSM investigation, the cleaning fluids were stained with Rhodamine 110 chloride (green, 27 μM). Moreover, Rhodamine B isothiocyanate (red, 19 μM) was encapsulated in the polymeric film in order to simultaneously and independently record the emission of both fluorescent probes and to obtain information on the interaction between the polymer and the cleaning fluids.

For atomic force microscopy (AFM), the binary and ternary fluids were diluted 10 times with water in order to slow down the removal process of the polymer film, which is thinner in this case (*vide infra*). It is worth noting that the diluted samples are still above the critical micellar concentration.

2.3. Small Angle X-ray Scattering (SAXS). Small-angle X-ray scattering experiments were performed at 25 °C with a HECUS S3-MICRO SWAXS-camera (Kratky) equipped with a position-sensitive detector (OED 50 M 1024 channels 54 μm wide). Cu Kα radiation of wavelength λ = 1.542 Å was provided by a GeniX X-ray generator

operating at a maximum power of 37 W. The sample-to-detector distance was 282 mm. The volume between the sample and the detector was kept under vacuum during the measurements to minimize the scattering from air. The Kratky camera was calibrated in the small angle region using silver behenate ($d = 58.38$ Å).[13] The samples were contained in 1.5 mm thick borosilicate capillary tubes sealed with hot melting glue. The scattering length density values (SLDs) were calculated for each component on the basis of its chemical composition and are reported in Table 2.

Table 2. Scattering Length Densities and Molecular Properties of the Chemicals Used in SAXS Experiments

compound	formula	molecular mass (g/mol)	SLD (10^{-6} Å^{-2})
water	H_2O	18.01	9.36
MEK	$(C_2H_5)CO(CH_3)$	72.11	7.47
SDS	$CH_3(CH_2)_{11}OSO_3Na$	288.35	9.22
SDS head	SO_4Na	119.02	22.4
SDS tail	$C_{12}H_{25}$	169.33	7.28

The X-ray scattering length density profile justifies a core–shell model for the micelles in which we can define three regions, each characterized by its own value of scattering length density: *bulk* (water), *core* (surfactant's tail), and *shell* (surfactant's head).

2.4. Atomic Force Microscopy (AFM). AFM measurements were performed with a PSIA XE-100E system. A 10% w/w solution of Paraloid B72 in ethyl acetate was deposited on top of glass substrates by spin coating (1000 rpm, 120 s). The thickness of the polymeric layer was then evaluated covering part of the glass slide with a Teflon tape before the spin coating process, finding a value of about 750 nm. 5 mL of liquid phase was put in contact with the substrates and allowed to interact for 3 and 8 h. To quench the interaction and freeze the morphology of the surface, the glass slides were quickly immersed in a large amount of water and allowed to dry. All the AFM images were acquired in noncontact mode (NCHR probes, radius of curvature at the tip of about 5 nm) on the dried films.

2.5. Confocal Laser Scanning Microscopy (CLSM). CLSM experiments were performed with a laser scanning confocal microscope Leica TCS SP2 (Leica Microsystems GmbH, Wetzlar, Germany) equipped with a 63× water immersion objective, using the 561 and 488 nm laser lines and by acquiring the fluorescent emission between 571–650 nm and 498–530 nm, respectively, for Rhodamine B isothiocyanate (codissolved with the polymer, red) and Rhodamine 110 chloride (dissolved in the aqueous liquid phase, green).

The substrates were coated with polymer films of different thicknesses using two procedures. Upon deposition of a droplet of a 10% w/w Paraloid B72 solution in acetone and evaporation of the solvent, a 30 μm thick film was obtained. Thinner films of about 6 μm were prepared by depositing a droplet of the same Paraloid B72 solution for spin coating (1000 rpm, 120 s). The polymer films are stained with Rhodamine B isothiocyanate, codissolved with the polymer solution in acetone. Then, 1 mL of the liquid phase labeled with Rhodamine 110 chloride was put in contact with the coated glass, and the morphological variations of the polymeric film were monitored as a function of time. In particular, thicker films were used to obtain high resolution images during the interaction between Paraloid B72 and the cleaning systems (water/MEK, BR/MEK 20%, and SDS/MEK 20%) while thinner films were employed to monitor the milder morphological variations induced by water and micellar solutions of both BR and SDS surfactants.

2.6. Contact Angle Measurements. The wetting properties of the polymer film were investigated by measuring the contact angle of 5 μL sessile droplets of Milli-Q water and of BR or SDS micellar solutions with a Ramé-Hart Model 190 CA Goniometer. The equilibrium contact angles were measured in four different areas on five different samples, and the average values and standard deviation were evaluated.

2.7. Cleaning Tests. Cleaning tests were performed on laboratory model samples (glass slides coated with Paraloid B72 300–500 μm thick films) using cellulose pulp poultices imbibed with the cleaning systems (application time: 1.5 and 3 h). At the end of the tests, the poultices were removed and the surface was gently rinsed with water to remove possible surfactant residues.

Although the thickness of polymer films is higher than in the case of CLSM (6 or 30 μm) and AFM (750 nm), the composition of the cleaning fluids is the same as the one used for CLSM. Therefore, the images acquired with confocal microscopy are representative of the real cases. Conversely, AFM measurements were performed after the dilution of the liquid media so that the observed morphological variations are most likely representative only of the first steps of polymer removal in real cases.

3. RESULTS AND DISCUSSION

3.1. Structural Characterization of the Nanofluids. Before addressing the interaction with the polymer film, we considered the structure of the liquid phases with particular attention to the partition of MEK, which has a water solubility of 275 g/L at 20 °C[14] between the continuous and the micellar phase. A structural characterization of BR/water/MEK systems, obtained through small-angle neutron scattering (SANS) and NMR self-diffusion, has recently been reported.[11] SDS-based formulations were investigated in this work through small-angle X-ray scattering (SAXS); Figure 2 shows the scattering profiles
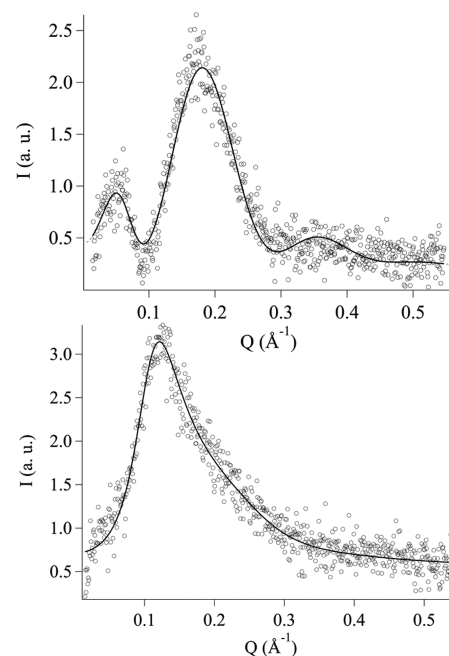

Figure 2. Top: scattering profile of SDS micelles (5%) in water; bottom: scattering profile of SDS micelles (4%) in the water/MEK (3.8:1) mixture. Fitting curves are reported as continuous lines together with the experimental data (empty circles).

obtained for SDS binary and ternary systems together with the best fitting curves. In both cases, a screened Coulomb potential was included in the fitting to account for intermicellar interactions.[15]

The main structural features obtained for BR and SDS/water binary systems are summarized in Table 3. BR aggregates in water can be modeled as polydisperse spherical micelles, in agreement with the previous literature on this nonionic class of surfactants.[16,17] On the other hand, SDS aqueous micelles can

Table 3. Main Fitting Parameters for BR-Based (SANS) and SDS-Based (SAXS) Formulations at 0% MEK Concentration

	0% MEK concentration (% w/w)	
	BR[f]	SDS
r (Å)[a]	16.6 ± 0.3	17.1 ± 0.1
Poly[b]	0.4 ± 0.1	0.12 ± 0.02
t (Å)[c]	7.7 ± 0.1	4.3 ± 0.1
N_w[d]	8.5	10
N_{agg}[e]	62	65

[a]r is the core radius. [b]Poly is the core polydispersity, expressed as a fraction of the unity [0, 1]. [c]t is the shell thickness. [d]N_w is the hydration number, i.e., the number of D_2O (BR) or H_2O (SDS) molecules included in the micelle shell per surfactant molecule. [e]N_{agg} is the average aggregation number. [f]From ref 11.

be conveniently modeled both as slightly elongated mono-disperse ellipsoids (up to 1.6 axial ratio), as reported in previously published SANS experiments,[18] or as slightly polydisperse spheres, as reported in the present work, to ease the comparison with the BR-based formulation. The length of the radius, r, plus the shell thickness, t, almost exactly matches the length of the fully extended molecule.[19−21] The effective charge (9.8, not reported in Tables 3 and 4), the hydration number (10), and the aggregation number (65) found in this paper are in agreement with the literature.[22,23]

Table 4. Main Fitting Parameters for BR-Based (SANS) and SDS-Based (SAXS) Formulations at 20% MEK Concentration

	20% MEK concentration (% w/w)	
	BR[g]	SDS
r (Å)[a]	14.1 ± 0.2	12.4 ± 0.5
Poly[b]	0.4 ± 0.1	0.3 ± 0.1
t (Å)[c]	4.5 ± 0.1	4.0 ± 0.4
N_w[d]	0.3	2.3
N_{agg}[e]	30	23
% MEK[f]	7.5 ± 2.5	25 ± 5

[a]r is the core radius. [b]Poly is the core polydispersity, expressed as a fraction of the unity [0, 1]. [c]t is the shell thickness. [d]N_w is the hydration number, i.e., the number of D_2O (BR) or H_2O (SDS) molecules included in the micelle shell per surfactant molecule. [e]N_{agg} is the average aggregation number. [f]% MEK is the amount of 2-butanone which penetrates inside the micelles' core. [g]From ref 11.

When 20% (w/w) MEK is added to the two systems, the micellar size decreases for both formulations (see Table 4). This behavior can be attributed to the interaction of MEK with the polar region of the aggregates (i.e., surfactant heads). The main difference between BR- and SDS-based formulations is the partition of the organic solvent between the bulk phase and the micelles.

In fact, MEK content is below the aqueous solubility limit for both systems but it scarcely penetrates the micellar structure of BR surfactant (about 5−10% of the total content is found associated with micelles) and remains mainly dissolved in the continuous medium. Conversely, in the case of SDS, there is a small yet appreciable MEK penetration in the aggregates: around 20−30% of the total amount is included in the micellar corona of SDS aggregates thanks to ion−dipole interactions between the charged head groups and the ketone group. In this case, MEK replaces H_2O, as suggested by the significant drop in

the hydration number, increasing the interfacial curvature and decreasing the average aggregation number to 23 SDS molecules per micelle. The different partition of the organic solvent between the bulk phase and the micellar core in BR and SDS systems might be responsible for the different cleaning performances for the two nanofluids.

3.2. Paraloid B72/Nanofluids Interaction. *3.2.1. Water on Paraloid B72 Films.* Water is a nonsolvent for Paraloid B72 and has no macroscopic effect on thick polymeric films. The low affinity between the film and water is confirmed by the contact angle (73° ± 3°), in line with the values usually found for hydrophobic polymer films.[24,25] However, on the nano- and microscale, the contact with water can induce morphological changes on the polymer surface, as found for PMMA (poly(methyl methacrylate)) films.[26,27] This effect should be considered in order to clarify the role of the additional components of the nanofluids at the same length scale.

The polymer surface has been observed after contact with water through AFM, frequently applied to monitor the effect of solvents and vapors on polymer films[28−31] and more recently to investigate the surface of cultural heritage artifacts to monitor surface cleaning processes.[6,32] After 3 h of incubation of a Paraloid B72 film with water, the simultaneous presence of pores with diameter and depth of about 10 nm and of protrusions from the surface occurs (Figure 3A). After contact
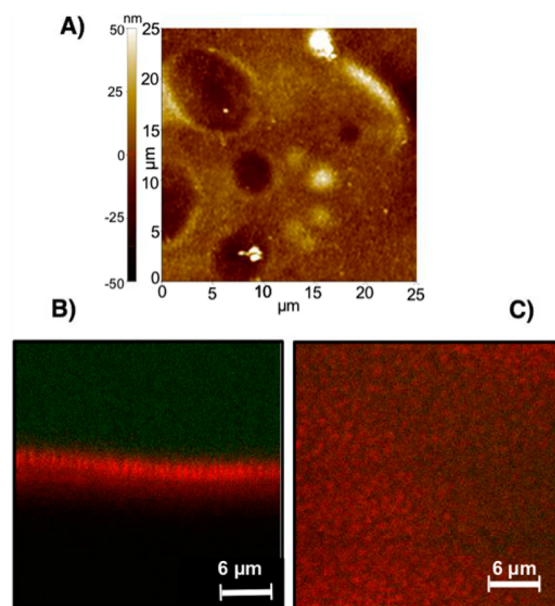

Figure 3. Paraloid B72 film on glass incubated with water for 3 h. (A) AFM image of a 750 nm thick film. CLSM vertical (B) and horizontal (C) sections of a 6 μm thick film. The polymeric film is stained with Rhodamine B isothiocyanate (red), while the liquid phase contains Rhodamine 110 chloride (green).

with water, the surface becomes rougher ($R_{rms} \sim$ 10 nm, compared to $R_{rms} \sim$ 0.7 nm before water addition). Overall, this suggests a structural reorganization induced by the presence of water and mediated by the hydrophobic nature of the polymer. Furthermore, the presence of protrusions on the surface might suggest a partial dissolution of minor components from the polymer film, which redeposit as the surface dries.

The AFM investigation was compared with an *in situ* CLSM observation of the whole process. A horizontal scan at the interface between the film and the liquid phase (Figure 3C),

recorded after 8 h, shows the formation of nanometric domains. These images are consistent with the limited changes observed at the macroscopic scale by the naked eye. Water hardly penetrates the film: the vertical scan (Figure 3B) shows that neither the green fluorescent tracer (dissolved in water) penetrates the polymeric film nor the red probe (encapsulated in the dried film, but also water-soluble) migrates toward the aqueous phase. Also in this case, water causes only the reorganization of the outer polymeric layers in contact with the polar fluid phase.

3.2.2. Surfactant Solutions on Paraloid B72 Films. The surface morphology of a Paraloid B72 film was also monitored after incubation with aqueous solutions of both nonionic (BR) and anionic (SDS) surfactants. Cleaning tests on laboratory models showed that, regardless of the application time and amphiphile nature, no polymer removal occurs with binary surfactant/water solutions.

Previous studies on thin PS (polystyrene) films proved the influence of surfactants used in the emulsion polymerization of styrene on the morphology of the film, on water penetration through defects and holes, and on dewetting properties.[33] Moreover, several groups have studied surfactant adsorption at the polymer/liquid interface. Usually, below the critical micellar concentration, strong cooperative adsorption is observed on hydrophilic surfaces, while a Langmuir trend is observed for hydrophobic noncrystalline surfaces.[34,35] Water swelling of the polymer film is enhanced by the presence of the surfactant, as monitored by neutron reflectivity for PS and PMMA films, while surfactant penetration in the film is not observed.[36] In our case, the attention was focused on the morphology of the polymer film and on its variations after exposure to the micellar solution, rather than on the presence and shape of surface aggregates.

3.2.2.1. BR/MEK 0%. The topographic AFM images of a Paraloid B72 film after contact with an aqueous solution of BR for 3 and 8 h, shown in Figure 4A,B, highlight the presence of surface protrusions, whose diameter and depth increase with time. Together with the larger pores, a population of smaller ones occurs, particularly visible for the sample exposed for 8 h.

The changes of surface morphology were confirmed through CLSM experiments. Here, the deformation of the polymer layer is clearly visible in the vertical section (Figure 4C). Interestingly enough, similarly to what is observed for neat solvents, the green fluorescent probe remains confined in the aqueous phase and the red tracer is not released by the film itself, indicating limited swelling. A comparison of Figure 4C,D indicates that the film is lifted from the glass substrate in a few round areas (darker circles in Figure 4D). This is a direct consequence of the surfactant presence, since no such effect is observed in neat water. The measured contact angle of BR/MEK 0% on the pristine film is $8° ± 1°$, confirming the enhanced wettability due to the presence of the nonionic surfactant.

3.2.2.2. SDS/MEK 0%. The AFM images of the polymer film exposed for 3 and 8 h to SDS micelles (Figure 5A,B, respectively) show the presence of small holes, irrespectively of the contact time with the liquid phase. Therefore, incubation of a Paraloid B72 film with an aqueous solution of SDS induces morphological variations on the polymeric film, but to a lesser extent with respect to those observed in the case of BR/MEK 0% solution. Moreover, the roughness of the film after incubation ($R_{rms} \sim 2.5$ nm) is similar to the initial one.

The weaker SDS effect is confirmed by CLSM investigation (Figure 5C,D), which reveals a slight deformation of the
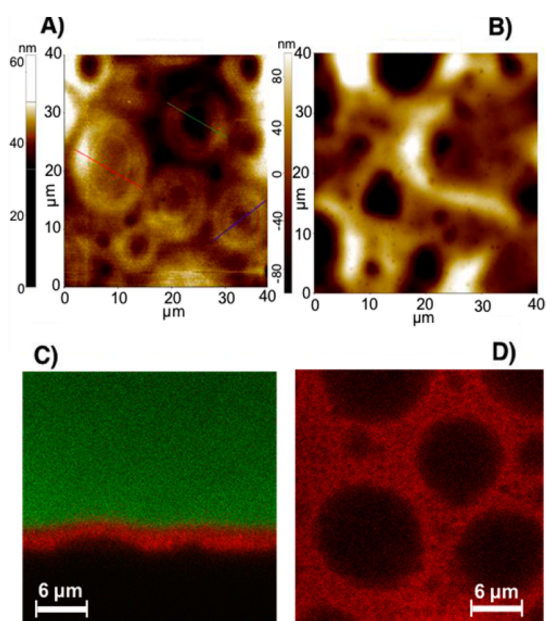

Figure 4. Paraloid B72 film deposited on glass incubated with a BR/MEK 0% mixture for 3 h (A) and 8 h (B) investigated by AFM. CLSM vertical (C) and horizontal (D) sections of a 6 μm thick film incubated for 8 h. The polymeric film is stained with Rhodamine B isothiocyanate (red), while the liquid phase contains Rhodamine 110 chloride (green).
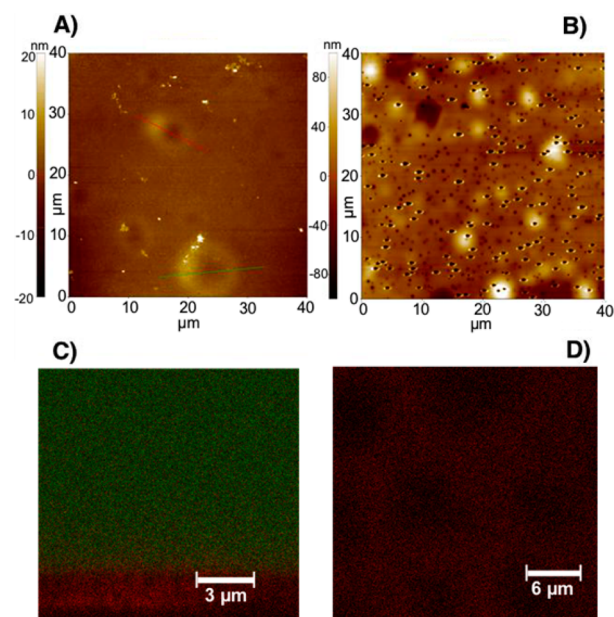

Figure 5. Paraloid B72 film deposited on glass incubated with a SDS/MEK 0% mixture for 3 h (A) and 8 h (B) investigated by AFM. CLSM vertical (C) and horizontal (D) sections of a 6 μm thick film incubated for 1.5 h. The polymeric film is stained with Rhodamine B isothiocyanate (red), while the liquid phase contains Rhodamine 110 chloride (green).

polymeric film with no substantial structural changes or polymer removal from the substrate. Further evidence of the different affinity of anionic and nonionic surfactant solutions toward the substrate is provided by the contact angle ($38° ± 1°$), considerably higher than that obtained for BR solutions.

A recent study on the adsorption of a series of nonionic alkyl polyglycolether surfactants (C_iE_j, where C_i stands for the number of carbons of the alkyl chain and E_j stands for the number of CH_2CH_2O units that are included in the polar head of the surfactant), containing different head groups onto hydrophobic solid−liquid interfaces, provided evidence that the adsorbed amount of surfactant decreases when an amide group, more hydrophilic than ethylene oxide, is present on the polar head.[37] In our case, BR is less hydrophilic, as is clear from the lower critical micellar concentration value with respect to SDS (0.9 mM vs 8.3 mM): it is therefore reasonable to expect a larger adsorption of BR at a hydrophobic interface, such as the Paraloid B72 one. In addition, the negative charge of the SDS polar heads might lower the saturation surface density due to electrostatic repulsion.

Contact angle measurements were performed also with BR/MEK 0% and SDS/MEK 0% solutions on Paraloid B72 films covered by physisorbed BR and SDS molecules. The films were exposed to the micellar solutions for 3 h to promote the adsorption of amphiphilic molecules on the polymer surface and then extensively washed with Milli-Q water to rinse off the excess surfactant.

The measured values were corrected taking into account the roughness induced on the polymeric surface after the incubation with the micellar solutions (see Figures 4A and 5A), according to the Wenzel equation:[38] $\cos \theta_W = r\cos \theta_Y$ where θ_W is the Wenzel apparent contact angle, θ_Y is the measured contact angle, and r is the roughness ratio, defined as the ratio of the true area of the solid surface to its nominal area and obtained from AFM. The obtained value is lower for the nonionic surfactant solution (i.e., $< 10°$ compared to $23° \pm 4°$ measured for SDS) confirming the higher affinity of BR for the hydrophobic chains of Paraloid B72, with respect to SDS. Table 5 reports all the values obtained from contact angle measurements already discussed in this section.

Table 5. Contact Angles of Water and Surfactants/Water Mixtures on Paraloid B72 Films

sample	contact angle (deg)
water	73 ± 3
BR/MEK 0%	8 ± 1
SDS/MEK 0%	38 ± 1
BR/water after BR absorption	<10
SDS/water after SDS absorption	23 ± 4

3.2.3. Water/MEK Mixture on Paraloid B72 Films. When a 500 μm polymer film laid on glass is left in contact with a mixture of water and MEK, which is a good solvent for Paraloid B72, laboratory cleaning tests show partial macroscopic swelling but no detachment from the substrate, also for long application times (3 h). This swelling, detected by the naked eye, can be appreciated at the nanoscale with AFM and CLSM. We remind that both investigations have been performed with films characterized by a lower thickness with respect to the cleaning tests.

AFM shows the formation of relatively large holes, with diameters of several microns and depths of about 100 nm (Figure 6A). The corresponding height profile shows that the deeper holes reach a maximum depth of about 500 nm compared to the initial thickness of the film (750 nm): we can conclude that, although the presence of MEK is responsible for the swelling and the structural reorganization of the polymer,

an ~200 nm polymer layer still persists on the glass surface. This is confirmed considering the value of the roughness inside a hole ($R_{rms} \sim 1$ nm), not significantly different from what is measured on the pristine polymer film ($R_{rms} \sim 0.7$ nm). This observation can be affected by the nature of the solid substrate, since the polymer chains in contact with it might establish H-bond interactions with the silanol groups on glass that are not overcome by the swelling operated by MEK.[39]

CLSM measurements were performed to follow *in situ* the modification of the polymeric film during the incubation with the water/MEK mixture. The vertical scan (Figure 6B) shows the presence of two simultaneous processes: swelling of external polymeric layers, indicated by a gradual release toward the bulk phase of the red tracer originally embedded in the film, and formation of yellow round areas at the glass/polymer interfacial region. As shown in Figure 6C (horizontal CLSM section at the film/liquid interface), these areas appear regularly shaped: the yellow color highlights the colocalization of the red and green probes, respectively, added to the polymeric film and to the liquid phase. We hypothesize the coexistence of solvents and polymer in these areas: in particular, it is likely that MEK (or a mixture of MEK and water) penetrates the entire thickness of the film, possibly through holes and channels, leading to the formation of a pattern, where regions composed of highly swollen polymer are included in a matrix of not-swollen glassy polymer.

3.2.4. Ternary Systems on Paraloid B72 Films. When water, MEK, and surfactant are combined, we obtain excellent cleaning performances, assessed by means of laboratory cleaning tests (see Table 6).[11] Clearly, it is the synergistic action of the three components that positively influences the cleaning process, even though the kinetics is different depending on the surfactant nature.

3.2.4.1. BR/MEK 20%. The AFM image recorded after 8 h (Figure 7A) shows strong morphological variations of the coating. In particular, we can identify large micrometric pores that almost reach the substrate with a depth of several hundreds of nanometers (as shown in the height profile, Figure 7A). However, the value of the roughness inside the holes ($R_{rms} \sim 1.2$ nm) is very close to that measured for the film before incubation ($R_{rms} \sim 0.7$ nm), indicating that a thin polymer film remains on the glass substrate. It is worthwhile to mention that the cleaning fluid was diluted 10 times for AFM investigation, as a consequence of the much lower thickness of the polymer film, with respect to laboratory cleaning tests. Therefore, the persistence of this thin layer of Paraloid B72 does not contradict the results of the cleaning tests, where complete removal of the polymeric coating is observed.

CLSM measurements were instead performed with the same concentrations used for the cleaning tests, and they are more representative for the real case; for incubation times longer than 35 min, no polymer is visible on the glass substrate. The horizontal section acquired at the film/glass interface after 30 min (Figure 7B) shows the penetration of the liquid phase inside the entire thickness of the polymeric film and the formation of green round-shaped areas similar to those observed for the water/MEK mixture. However, in this case, no colocalization of the fluorescent probes respectively embedded in the film (red) and dissolved the liquid phase (green) is observed. This can be explained because the removal process is relatively fast, when compared to water/MEK, and it is consistent with the segregation of the fluorescent labels in the aqueous phase and in the polymer film. Moreover, differently
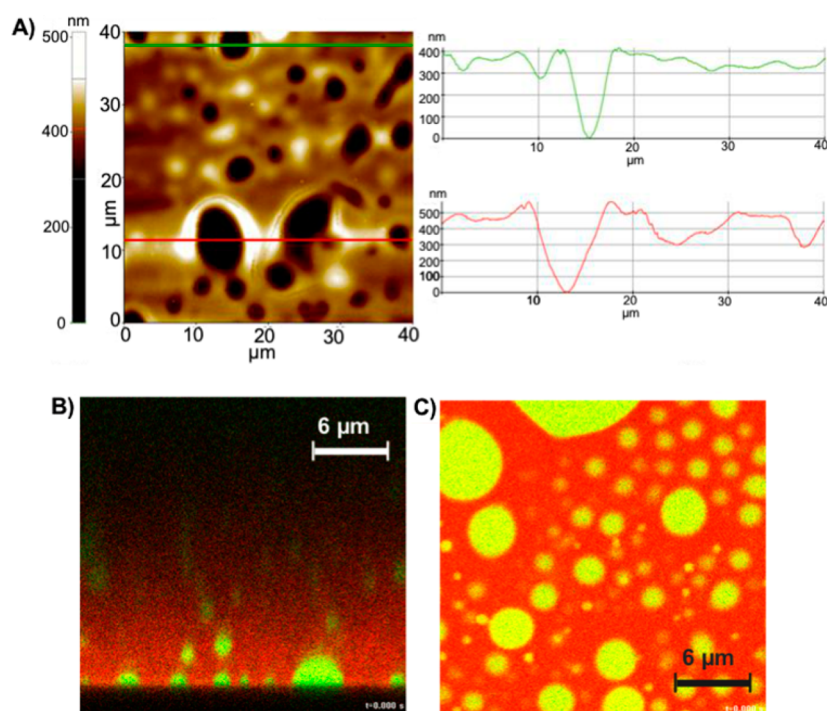
Figure 6. Paraloid B72 film deposited on glass incubated with a water/MEK mixture for 3 h: AFM image (A) of a 750 nm thick film. The height profile along two lines is also reported. CLSM vertical (B) and horizontal (C) sections of a 30 μm thick film incubated for 30 min. The polymeric film is stained with Rhodamine B isothiocyanate (red), while the liquid phase contains Rhodamine 110 chloride (green).

Table 6. Polymer Removal (Reported as % w/w with Respect to the Polymer Mass Originally Present on Each Glass Slide) after 1.5 and 3 h of Exposure to BR and SDS Ternary Systems Containing 20% of MEK

	polymer removal (% w/w)	
sample	1.5 h	3 h
BR/MEK 20%	86 ± 2	99 ± 3
SDS/MEK 20%	0 ± 10	100 ± 1

from what was observed with the water/MEK solution, the round green areas at the glass/liquid interface rapidly coalesce giving rise to irregular structures. Clearly, the presence of the surfactant guarantees a decrease of the interfacial tension between the glass and the swollen polymer droplets and, therefore, the stabilization of these irregular structures.

The main evidence of polymer removal comes from the CLSM horizontal scan acquired at about one-half of the initial thickness of the polymer film (Figure 7C). By following the Rhodamine B isothiocyanate emission, it appears that small droplets of swollen polymer are formed while the surrounding polymer matrix appears disrupted. We hypothesize that the surfactant has a role also in the interfacial stabilization of these droplets and, therefore, enhances polymer dewetting.

3.2.4.2. SDS/MEK 20%. The topographical AFM images of the polymeric film (Figure 8A,B) show that small holes with a maximum depth of about 100 nm appear only for long incubation times (8 h): this confirms that SDS has weaker interactions with the film with respect to BR surfactant, as is already discussed for the binary systems. However, despite the different affinity of the two surfactants for the polymeric coating, the molecular mechanism followed by means of CLSM investigations is similar in both cases.

The horizontal scan acquired at the glass/polymer interface (Figure 8C) after 1.5 h shows the formation of green round areas that may be interpreted as containing only the liquid phase, similarly to what was found for BR/MEK 20%. The main difference is that the horizontal scan acquired at about one-half of the initial thickness (Figure 8D) does not reveal the presence of droplets of swollen polymer: the SDS-based ternary system, while penetrating through the entire thickness of the film, deforms the polymer in contact with the substrate but removes only the outer layers of the film in direct contact with the liquid phase.

Combining the results discussed so far, a possible explanation of the particular behavior observed for the ternary system with respect to the other formulations is a cooperative mechanism among the three components of the nanofluid. We can thus distinguish the main steps of the interaction between the polymer film and the liquid phase, also underlining the specific function carried out by each component (Figure 9), as follows: (1) Water interacts with the outer layers of the polymer causing its structural reorganization. (2) The organic solvent (MEK) in the continuous aqueous phase, in equilibrium with that confined inside the micelles, quickly swells the external polymeric layers. In particular, the polymer undergoes relevant structural changes when MEK in the bulk phase reaches a "critical concentration". This can be confirmed by looking at the poor cleaning performances shown by SDS/MEK 20% (especially for short application times of 1.5 h), where a not negligible amount of MEK is confined inside the micellar core, compared to those of a BR-based ternary system, in which a larger amount of organic solvent is available in the bulk. Furthermore, cleaning tests performed in our previous work[11] with ternary systems containing 13.5% (w/w) of MEK and both surfactants show weak performances with respect to the 20% MEK system, even for long application times (see Table
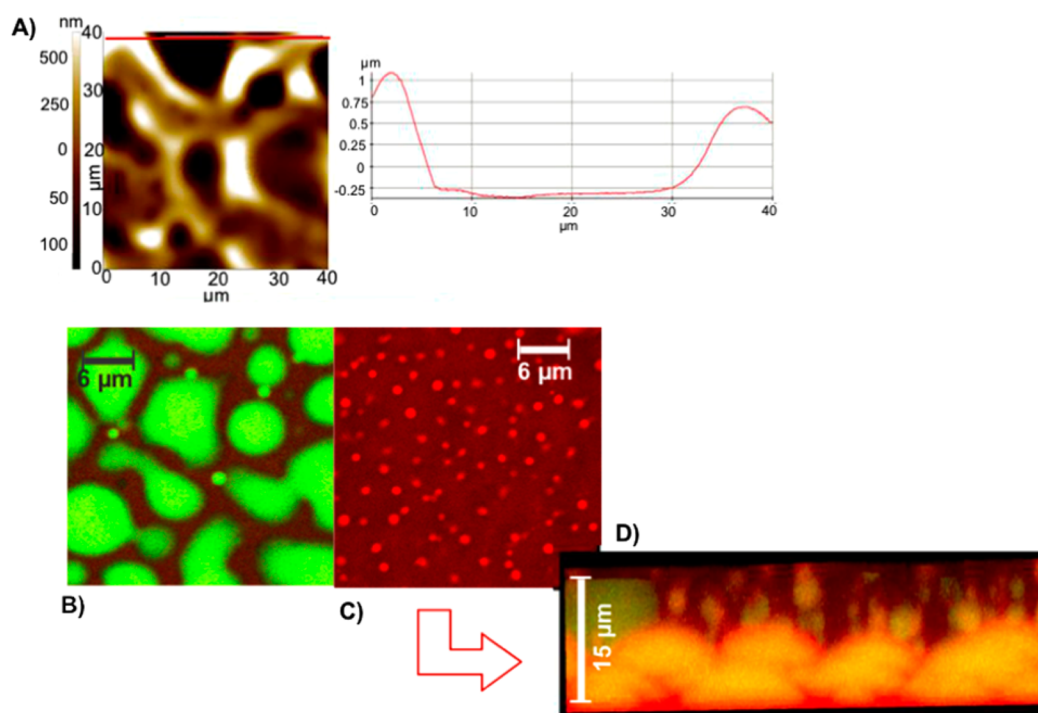
Figure 7. Paraloid B72 film deposited on glass incubated with ternary system BR/MEK 20% for 8 h (A) investigated by AFM. Horizontal CLSM scan at the polymer/glass interface (B), horizontal CLSM scan at about one-half of the initial thickness (C) where only the fluorescence of the probe encapsulated into the polymer is recorded, and CLSM 3D section (D) of a 30 μm thick film incubated for 30 min. The polymeric film is stained with Rhodamine B isothiocyanate (red), while the liquid phase contains Rhodamine 110 chloride (green).
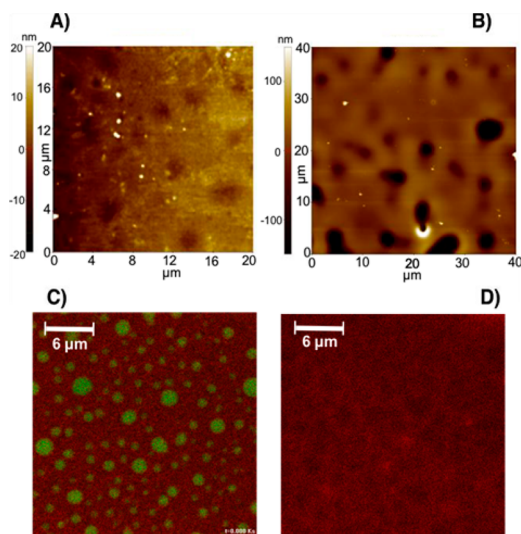

Figure 8. Paraloid B72 film deposited on glass incubated with SDS/ MEK 20% for 3 h (A) and 8 h (B) investigated by AFM. Horizontal CLSM scan at the interface polymer/glass (C) and horizontal CLSM scan at about one-half of the initial thickness (D) section of a 30 μm thick film incubated for 1.5 h. The polymeric film is stained with Rhodamine B isothiocyanate (red), while the liquid phase contains Rhodamine 110 chloride (green).

7). (3) The amphiphilic molecules move from the bulk to the polymer surface where they adsorb more or less efficiently depending on their chemical nature and affinity for Paraloid B72. The interaction between the polymer and the surfactant promotes some surface morphological reorganization. (4) MEK penetrates within the inner polymeric layers of the polymer film swelling them and driving the polymer dewetting. The polymer

detaches from the glass substrate thanks to the key role played by the surfactant in the removal process. In fact, it decreases the polymer/glass surface tension favoring the detachment of swollen polymer droplets from the glass substrate.

4. CONCLUSIONS

This study reports the combined use of optical techniques, such as confocal laser scanning microscopy, and surface methods (atomic force microscopy, contact angle) to understand the mechanism occurring during the removal of a hydrophobic polymer film (Paraloid B72) from solid surfaces with nanostructured cleaning media. The nanofluids presented here are constituted by a nonionic surfactant, water, and MEK (a nonsolvent and a good solvent for the polymer, respectively). These systems possess interesting properties due to the biocompatibility and eco-sustainability of the surfactant and to the excellent cleaning performances assessed with laboratory tests on glass slides and model and *real* fresco paintings, where a polymeric coating had been previously applied. A comparison with a similar three-component system containing an anionic surfactant (SDS) is presented to investigate the influence of the surfactant structure on the removal process.

Cleaning tests, coupled with the direct observation of the morphological changes of the polymer film by means of CLSM and AFM analysis, have shown that the nonionic surfactant is more efficient in polymer removal than SDS, the concentration of MEK being constant. We suggest that this behavior is related to the charge and hydrophilicity of SDS, which disfavors the adsorption of surfactant micelles on the external layers of the polymeric coating, and to the different partition of MEK between the bulk phase and the micellar core. In fact, SANS and SAXS analyses evidenced that MEK is mainly dissolved in
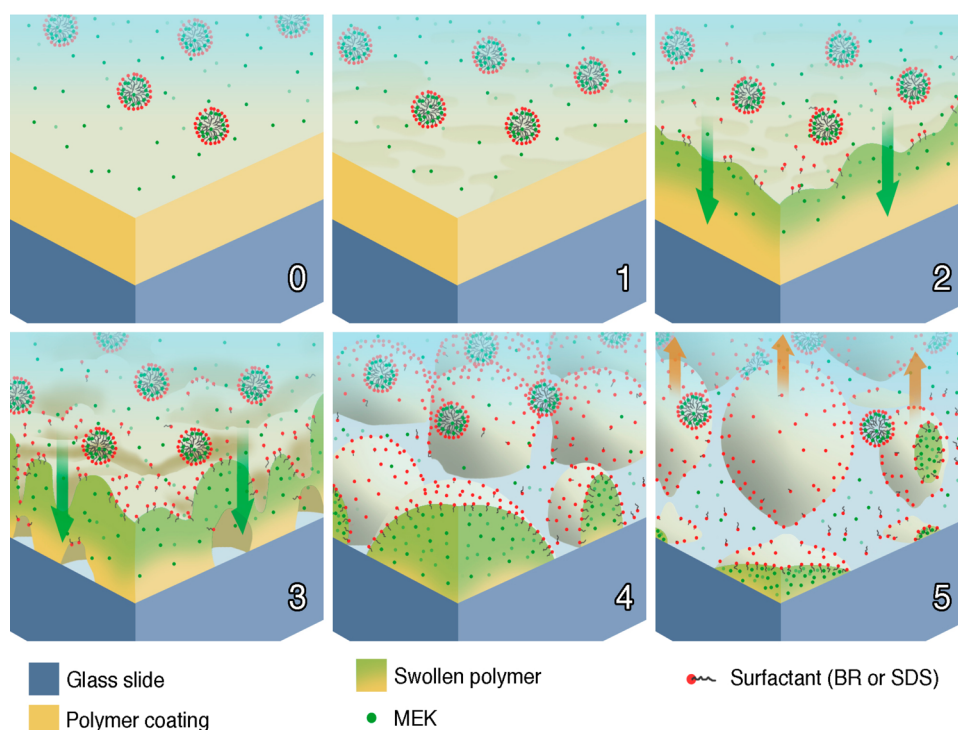
Figure 9. Schematic representation of the mechanism of interaction between the nanofluid and the polymeric coating. (0) Polymeric coating put in contact with the nanofluid. (1) Structural reorganization of the polymer induced by water. (2) MEK quickly swells the external polymeric layers. (3) Amphiphilic molecules adsorb on the swollen polymer and promote some surface morphological reorganization. (4) MEK penetrates within the film causing its swelling. (5) Polymer detaches from the glass substrate.

Table 7. Polymer Removal (Reported as % w/w with Respect to the Polymer Mass Originally Present on Each Glass Slide) after 1.5 and 3 h of Exposure to BR- and SDS-Based Formulations Containing 13.5% of MEK

	polymer removal (% w/w)	
sample	1.5 h	3 h
BR/MEK 13.5%	43 ± 5	100 ± 2
SDS/MEK 13.5%	0 ± 10	0 ± 10

the aqueous bulk phase for both BR/MEK 20% and SDS/MEK 20%; nevertheless, about 20−30% of the total amount of the organic solvent penetrates inside the SDS micellar phase while only 5−10% of MEK is confined in BR micelles. These structural differences can be responsible for the different cleaning efficacies and for the different kinetic profiles observed; however, our results indicate some common key steps.

In particular, the synergistic action between water, MEK, and surfactant is of fundamental importance to obtain excellent cleaning performances. In fact, water causes the structural reorganization of the external polymeric layers while the organic solvent swells the entire film increasing the mobility of the polymeric chains. At the same time, the surfactant interacts with the outer polymeric layers and decreases the interfacial energy at the glass/polymer interface, promoting the detachment of the polymer from the glass substrate.

■ AUTHOR INFORMATION

Corresponding Authors
*E-mail: piero.baglioni@unifi.it. Phone: +390554573033.
*E-mail: berti@csgi.unifi.it. Phone: +390554573038.

Author Contributions
The manuscript was written through contributions of all authors. All authors have given approval to the final version of the manuscript.

Notes
The authors declare no competing financial interest.
[†]M. Baglioni and P. Baglioni: No kinship exists between the authors.

■ REFERENCES

(1) Carretti, E.; Dei, L. Physicochemical Characterization of Acrylic Polymeric Resins Coating Porous Materials of Artistic Interest. *Prog. Org. Coat.* **2004**, *49*, 282−289.

(2) Horie, C. V. *Materials for Conservation: Organic Consolidants, Adhesives and Coatings*, 2nd ed.; Butterworth-Heinemann: Amsterdam; Boston, 2010.

(3) Favaro, M.; Mendichi, R.; Ossola, F.; Russo, U.; Simon, S.; Tomasin, P.; Vigato, P. A. Evaluation of Polymers for Conservation Treatments of Outdoor Exposed Stone Monuments. Part I: Photo-Oxidative Weathering. *Polym. Degrad. Stab.* **2006**, *91*, 3083−3096.

(4) Giorgi, R.; Baglioni, M.; Berti, D.; Baglioni, P. New Methodologies for the Conservation of Cultural Heritage: Micellar Solutions, Microemulsions, and Hydroxide Nanoparticles. *Acc. Chem. Res.* **2010**, *43*, 695−704.

(5) Carretti, E.; Giorgi, R.; Berti, D.; Baglioni, P. Oil-in-Water Nanocontainers as Low Environmental Impact Cleaning Tools for Works of Art: Two Case Studies. *Langmuir* **2007**, *23*, 6396−6403.

(6) Baglioni, M.; Rengstl, D.; Berti, D.; Bonini, M.; Giorgi, R.; Baglioni, P. Removal of Acrylic Coatings from Works of Art by Means of Nanofluids: Understanding the Mechanism at the Nanoscale. *Nanoscale* **2010**, *2*, 1723−1732.

(7) Baglioni, M.; Giorgi, R.; Berti, D.; Baglioni, P. Smart Cleaning of Cultural Heritage: A New Challenge for Soft Nanoscience. *Nanoscale* **2012**, *4*, 42−53.

(8) Carretti, E.; Fratini, E.; Berti, D.; Dei, L.; Baglioni, P. Nanoscience for Art Conservation: Oil-in-Water Microemulsions Embedded in a Polymeric Network for the Cleaning of Works of Art. *Angew. Chem., Int. Ed. Engl.* **2009**, *48*, 8966−8969.

(9) Baglioni, P.; Berti, D.; Bonini, M.; Carretti, E.; Dei, L.; Fratini, E.; Giorgi, R. Micelle, Microemulsions, and Gels for the Conservation of Cultural Heritage. *Adv. Colloid Interface Sci.* **2014**, *205*, 361−371.

(10) Baglioni, P.; Chelazzi, D.; Giorgi, R.; Poggi, G. Colloid and Materials Science for the Conservation of Cultural Heritage: Cleaning, Consolidation, and Deacidification. *Langmuir* **2013**, *29*, 5110−5122.

(11) Baglioni, M.; Raudino, M.; Berti, D.; Keiderling, U.; Bordes, R.; Holmberg, K.; Baglioni, P. Nanostructured Fluids from Degradable Nonionic Surfactants for the Cleaning of Works of Art from Polymer Contaminants. *Soft Matter* **2014**, *10*, 6798−6809.

(12) Carretti, E.; Dei, L.; Baglioni, P. Solubilization of Acrylic and Vinyl Polymers in Nanocontainer Solutions. Application of Microemulsions and Micelles to Cultural Heritage Conservation. *Langmuir* **2003**, *19*, 7867−7872.

(13) Blanton, T. N.; Huang, T. C.; Toraya, H.; Hubbard, C. R.; Robie, S. B.; Louër, D.; Göbel, H. E.; Will, G.; Gilles, R.; Raftery, T. JCPDS—International Centre for Diffraction Data Round Robin Study of Silver Behenate. A Possible Low-Angle X-Ray Diffraction Calibration Standard. *Powder Diffr.* **2013**, *10*, 91−95.

(14) Stephenson, R. M. Mutual Solubilities: Water-Ketones, Water-Ethers, and Water-Gasoline-Alcohols. *J. Chem. Eng. Data* **1992**, *37*, 80−95.

(15) Baglioni, M.; Berti, D.; Teixeira, J.; Giorgi, R.; Baglioni, P. Nanostructured Surfactant-Based Systems for the Removal of Polymers from Wall Paintings: A Small-Angle Neutron Scattering Study. *Langmuir* **2012**, *28*, 15193−15202.

(16) Glatter, O.; Fritz, G.; Lindner, H.; Brunner-Popela, J.; Mittelbach, R.; Strey, R.; Egelhaaf, S. U. Nonionic Micelles near the Critical Point: Micellar Growth and Attractive Interaction. *Langmuir* **2000**, *16*, 8692−8701.

(17) Gapiński, J.; Szymański, J.; Wilk, A.; Kohlbrecher, J.; Patkowski, A.; Hołyst, R. Size and Shape of Micelles Studied by Means of SANS, PCS, and FCS. *Langmuir* **2010**, *26*, 9304−9314.

(18) Colafemmina, G.; Fiorentino, D.; Ceglie, A.; Carretti, E.; Fratini, E.; Dei, L.; Baglioni, P.; Palazzo, G. Structure of SDS Micelles with Propylene Carbonate as Cosolvent: A PGSE-NMR and SAXS Study. *J. Phys. Chem. B* **2007**, *111*, 7184−7193.

(19) Cabane, B. Small Angle Scattering Methods. In *Surfactant Solutions New Methods of Investigation*; Zana, R. E., Ed.; Marcel Dekker, Inc.: New York, 1987.

(20) Cabane, B. Growth: A Brief Guide for the Use of Scattering Techniques. In *Neutron, X-Ray and Light Scattering as Investigative Tools for Colloidal and Polymeric Systems*; Lindner, P., Zemb, T., Eds.; Elsevier: Amsterdam, 1991.

(21) Tanford, C. *The Hydrophobic Effect: Formation of Micelles and Biological Membranes*; Wiley: New York, 1980.

(22) Sheu, E. Y.; Chen, S. H. Thermodynamic Analysis of Polydispersity in Ionic Micellar Systems and Its Effect on Small-Angle Neutron-Scattering Data Treatment. *J. Phys. Chem.* **1988**, 4466−4474.

(23) Caponetti, E.; Chillura Martino, D.; Floriano, M. A.; Triolo, R. Localization of N-Alcohols and Structural Effects in Aqueous Solutions of Sodium Dodecyl Sulfate. *Langmuir* **1997**, 3277−3283.

(24) Gilchrist, V. A.; Lu, J. R.; Keddie, J. L.; Staples, E.; Garrett, P. Adsorption of Penta(ethylene Glycol) Monododecyl Ether at the Solid Poly(methyl methacrylate)−Water Interface: A Spectroscopic Ellipsometry Study. *Langmuir* **2000**, *16*, 740−748.

(25) Johnson, B. A.; Kreuter, J.; Zografi, G. Effects of Surfactants and Polymers on Advancing and Receding Contact Angles. *Colloids Surf.* **1986**, *17*, 325−342.

(26) Tanaka, K.; Fujii, Y.; Atarashi, H.; Akabori, K.; Hino, M.; Nagamura, T. Nonsolvents Cause Swelling at the Interface with Poly(methyl Methacrylate) Films. *Langmuir* **2008**, *24*, 296−301.

(27) Tateishi, Y.; Kai, N.; Noguchi, H.; Uosaki, K.; Nagamura, T.; Tanaka, K. Local Conformation of Poly(methyl Methacrylate) at Nitrogen and Water Interfaces. *Polym. Chem.* **2010**, *1*, 303.

(28) Sinturel, C.; Vayer, M.; Morris, M.; Hillmyer, M. A. Solvent Vapor Annealing of Block Polymer Thin Films. *Macromolecules* **2013**, *46*, 5399−5415.

(29) Magonov, S. N. Atomic Force Microscopy in Analysis of Polymers. In *Encyclopedia of Analytical Chemistry*; John Wiley & Sons, Ltd: Chichester, UK, 2000.

(30) Bang, J.; Kim, B. J.; Stein, G. E.; Russell, T. P.; Li, X.; Wang, J.; Kramer, E. J.; Hawker, C. J. Effect of Humidity on the Ordering of PEO-Based Copolymer Thin Films. *Macromolecules* **2007**, *40*, 7019−7025.

(31) Cong, Y.; Zhang, Z.; Fu, J.; Li, J.; Han, Y. Water-Induced Morphology Evolution of Block Copolymer Micellar Thin Films. *Polymer* **2005**, *46*, 5377−5384.

(32) Pereira, C.; Ferreira, I. M. P. L. V. O.; Branco, L. C.; Sandu, I. C. A.; Busani, T. Atomic Force Microscopy as a Valuable Tool in an Innovative Multi-Scale and Multi-Technique Non-Invasive Approach to Surface Cleaning Monitoring. *Procedia Chem.* **2013**, *8*, 258−268.

(33) Castro, L. B. R.; Almeida, A. T.; Petri, D. F. S. The Effect of Water or Salt Solution on Thin Hydrophobic Films. *Langmuir* **2004**, *20*, 7610−7615.

(34) Fragneto, G.; Lu, J. R.; McDermott, D. C.; Thomas, R. K.; Rennie, A. R.; Gallagher, P. D.; Satija, S. K. Structure of Monolayers of Tetraethylene Glycol Monododecyl Ether Adsorbed on Self-Assembled Monolayers on Silicon: A Neutron Reflectivity Study. *Langmuir* **1996**, *12*, 477−486.

(35) Tiberg, F.; Brinck, J.; Grant, L. Adsorption and Surface-Induced Self-Assembly of Surfactants at the Solid-Liquid Interface. *Curr. Opin. Colloid Interface Sci.* **2000**, 411−419.

(36) Howse, J. R.; Steitz, R.; Pannek, M.; Simon, P.; Schubert, D. W.; Findenegg, G. H. Adsorbed Surfactant Layers at Polymer/Liquid Interfaces. A Neutron Reflectivity Study. *Phys. Chem. Chem. Phys.* **2001**, *3*, 4044−4051.

(37) Kjellin, U. R. M.; Claesson, P. M.; Linse, P. Surface Properties of Tetra(ethylene Oxide) Dodecyl Amide Compared with Poly(ethylene Oxide) Surfactants. 1. Effect of the Headgroup on Adsorption. *Langmuir* **2002**, *18*, 6745−6753.

(38) Marmur, A. Wetting on Hydrophobic Rough Surfaces: To Be Heterogeneous or Not To Be? *Langmuir* **2003**, *19*, 8343−8348.

(39) Xue, L.; Han, Y. Autophobic Dewetting of a Poly(methyl Methacrylate) Thin Film on a Silicon Wafer Treated in Good Solvent Vapor. *Langmuir* **2009**, *25*, 5135−5140.